N70-27419

NASA TECHNICAL TRANSLATION NASA TT F12,753

DESCRIPTION AND EFFECT OF UNSTEADY GUST DERIVATIVES OF THE LONGITUDINAL MOTION OF AN AIRCRAFT

G. Schanzer

Translation of "Beschreibung und Auswirkung Instationärer Böenderivativa der Flugzeuglängsbewegung". Paper presented at the annual Meeting of the Deutsche Gesellschaft für Luft- und Raumfahrt, Bremen, West Germany, Sept. 22 - 24, 1969, 42 pages

CASE FILE COPY

NATIONAL AERONAUTICS AND SPACE ADMINISTRATION
WASHINGTON, D.C. 20546 MAY 1970

TABLE OF CONTENTS

		Page
1.	Introduction	2
	1.1 Introduction	2
	1.2 Summary	3
2.	Designation	3
3.	Quasi-stationary gust effects	5
	3.1 Dead time effects as a result of delayed flow processes	5
	3.2 Dead time effects as a result of angle of attack and downwash delays	7
	3.3 Dead time effects as a result of thrust velocity delays	12
	3.4 Summarizing remarks on the gust derivatives	15
	3.5 Physical action of the dead time effect	16
	3.6 Region of validity for the quasi-stationary derivatives	17
4.	Effects of instantaneous gusts on the aircraft longitudinal motion	17
	4.1 All-pass effects	18
	4.2 Dead time behavior as a result of all-pass effects	19
	4.3 Typical qualities of $c_{M\dot{\alpha}}$ and $c_{M\dot{w}w}$	20
	4.3.1 Variation of $c_{M\dot{\alpha}w}$	20
	4.3.2 Variation of $c_{M\dot{w}w}$	22
5.	Some effects of the Nonsteady gust effect on the flight control systems	22
6.	Summary	24
7.	References	26

DESCRIPTION AND EFFECT OF UNSTEADY GUST DERIVATIVES OF THE LONGITUDINAL MOTION OF AN AIRCRAFT

G. Schanzer

ABSTRACT. Analysis of unsteady flows caused by rough air and their effect on the longitudinal motion of an aircraft and on flight stability and control. It is shown that a quasi-steady-state method of investigation is sufficient for the relatively slow motion of the aircraft in the direction of its flight. Quasi-steady-state parameters are derived for horizontal and vertical effects of rough air. The effect of vertical and horizontal perturbations is discussed for aircraft types similar to the Boeing 707 and to the Concorde.

Summary

After an evaluation of gust power spectra, it is shown that for relatively/5* slow flight path motion of an aircraft a quasi-stationary consideration is sufficient. For horizontal and vertical gust effects, quasi-stationary derivatives are deduced and compared with the previously known quasi-stationary derivatives $c_{M\dot{\alpha}}$ and c_{My}, as well as with variable calculations.

$$c_{M\dot{\alpha}_w} = c_{M\dot{\alpha}} - c_{My}$$

$$c_{M\hat{w}} = -2\,\frac{c_{A(H)}}{c_{A\alpha(H)}}\,c_{My}$$

The effect of vertical and horizontal gust perturbations on the aircraft longitudinal motion, in particular the all-pass effects caused through intermittent flow processes, are discussed for two example aircraft with the aid of fundamental diagrams and transient solutions.

---

* Numbers in the margin indicate pagination in the original foreign text.

1. Introduction

1.1 Introduction

The flight properties of an aircraft are strongly affected by its natural /7
oscillation behavior and its reaction to external perturbations (e.g., gusts). In order to be able to determine the flight characteristics, such as, for example, good controllability, passenger comfort, adherence to the flight path, and speed, it is neccessary to have exact knowledge of the system of motion equations that describes the flight motion of the aircraft. This knowledge is particularly important if an automatic pilot is to be used to improve the flight characteristics.

The most important external perturbations which affect the aircraft are gusts and cross winds. They may be described by a time-dependent velocity vector with reference to the aircraft center of gravity. It can be resolved into components parallel to the direction of the flight path (change of the thrust velocity $u_w(t)$) and perpendicular to it (change of the angle of attack $\alpha_w(t)$). The quantities $\alpha_w(t)$ and $u_w(t)$ are stochastic functions [1]. Their high-frequency components can bring about intermittent flow processes on the wing and tail assembly. Since the frequency of gust occurrence increases in proportion to the flight speed [1], the effective gust frequencies at the relatively low speeds of the landing approach are proportionately low. In this case, one can make a simplifying assumption that no significant phase shifts occur between the air forces on the wing and the attacking gust perturbations; that is, there is a fixed relation between the changes of attack angle and the thrust velocity, on the one hand and the air forces, on the other hand. However, retardation of the wing downwash to the horizontal tail surfaces must be considered, since it would cause a significant pitch moment. Since the effective gust frequencies [2] — cross winds included — in the landing approach are low, the pitch moments caused by intermittent flow processes may be quite nearly approximated through quasi-stationary statements, and may be described

by simple explicit formulas.[1]

1.2 Summary

Aerodynamic effects on the aircraft motion equations are described through transfer functions. Usually only the constant term of this transfer function is determined in wind tunnel measurements. For dynamic processes, to a first approximation at least, a time-dependent term should also be determined, since the aircraft motion equations are strongly affected by it. These time-dependent terms are inherently difficult to determine, and it is shown how they may be approximately calculated from other known characteristic quantities. /8

Besides the description of the intermittent flow processes caused by gusts, their effects on the aircraft longitudinal motion for two example aircraft will be discussed in particular. Thus, it is shown that in many cases intermittent flow processes amplify the undesirable effects of cross winds. The consequences of this on some common controller principles are discussed with reference to construction of flight controllers, e.g. BLEU (an automatic landing system) and thrust controllers.

2. Designations

These designations correspond basically with LN 9300. Additions to, or deviations from, LN 9300 are defined: /9

α	angle of attack
ϑ	longitudinal course angle
γ	flight path angle
U	flight path velocity
V	thrust velocity (air speed)
U_w	gust velocity in the flight path direction
W_w	gust velocity perpendicular to the flight path direction

[1] These formulas were confirmed for a simple uncambered delta wing in non-steady flow with the aid of the theory of slender bodies [3].

$u = \frac{U-U_o}{U_o}$	relative flight path velocity
$v = \frac{V-V_o}{V_o}$	relative thrust velocity
$u_w = \frac{U_w}{U_o}$	relative gust velocity parallel to flight path
$\alpha_w = \frac{-W_w}{U_o}$	increase in angle of attack as a result of a gust perpendicular to the flight direction
$t_a = \frac{l_\mu}{U_o}$	aerodynamic time unit
$i_y = \frac{2 I_y}{\rho F l_\mu^3}$	dimensionless moment of inertial around the aircraft roll axis
$\varepsilon = \frac{\partial \alpha_w}{\partial \alpha}$	downwash gradient on the horizontal tail assembly
w_i	downwash on the horizontal tail assembly
λ	gust wave length
ω_g	gust limiting frequency
ω_y	pitch angular velocity
x_S	position of the center of gravity, measured outward from the leading edge of the wing

Indices:

A	lift
W	drag
w	wind (gust)
y	around the aircraft roll axis
H	horizontal tail assembly
FL	wing
o	fixed initial state

3. Quasi-stationary gust effects

3.1 Dead time effects as a result of delayed flow processes. /10

The quasi-stationary effects arise from temporary changes in local flow processes produced by fluctuation in the angle of attack or thrust velocity, which have a time-delayed effect in the flow direction. The physical process will be explained with a simplified model. After a sudden increase of the wing's attack angle, its circulation increases by $\Delta\Gamma$. An oppositely rotating initial vortex with the same magnitude of $\Delta\Gamma$ separates at the velocity of the air stream from the initial direction, because the sum of the newly forming vortices must be zero, according to the Helmholtz law of vortices. Figure 1 shows the vortex system for a wing-elevator combination at a fixed point in time.

In Figure 2 the solid curve shows the temporal division of the downwash at the location of the horizontal tail surface. This results from the additional circulation and from the initial vortex being washed away at the velocity V of the initial air stream. This time function is approximated by a step function with dead time Δt (dashed line in Figure 2) which shows clearly the delay of the downwash.

$$\Delta t = \frac{r_H}{V} \tag{1}$$

Thus r_H is the separation between the neutral points of the wing and the tail assembly.

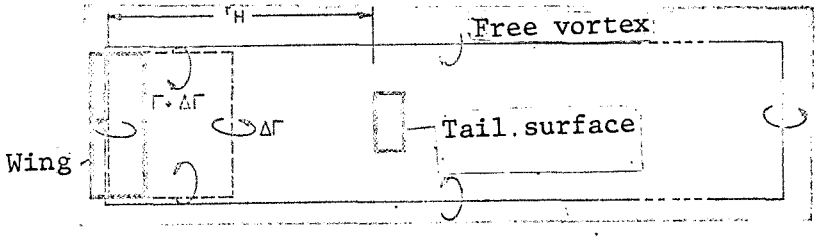

Figure 1

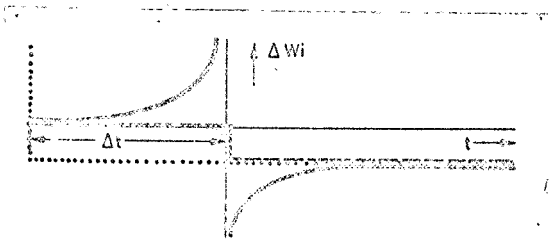

Figure 2

The step function with dead time[2] may be replaced by a quasi-stationary approximation corresponding to Equation (2) (dotted line in Figure 2).

$$c_M = c_{M\alpha}\alpha + c_{M\dot{\alpha}}\dot{\alpha} \qquad (2)$$

Figure 2 shows that this approximation /11 is meaningful only for $t >> \Delta t$; i.e., changes in flow processes shortly after occurence of the perturbation must remain unconsidered.

Thus, the postulates for a quasi-stationary viewpoint are fulfilled. For this reason only, the steady-state condition ($t >> \Delta t$) can be considered with constant rate of change using ramp functions, which serve well for representation of quasi-stationary processes (e.g., cross winds).

With the circulation changes on the wing, discussed above, and their effect on the horizontal tail surface[3] four cases of flight-mechanical interest may be resolved. They will subsequently be investigated.

The commonly known determination of $c_{M\dot{\alpha}}$ (case 1) will serve here as an introduction to this viewpoint. With it, estimates are made possible, and differences are noted.

The following investigations are discussed for a simplified two-dimensional /12

---

[2] An example of a transfer function with dead time is $c_M/\alpha = Ke^{-s\Delta t}$. The development of this complex exponential function leads to a PD-term with a positive zero position $c_M/\alpha \approx K(1 - s\Delta t)$. The Padé approximation [4] serves as a still better approximation for a transfer function with dead time. Here the dead time behavior is simulated by a combination of all-pass and delay terms [5]. Hamel [6] has shown that the series development may be terminated at two terms and still give sufficient accuracy for the relatively low characteristic frequencies of the longitudinal motion for a rigid aircraft.

[3] The delayed flow processes occur in a similar form with a flying wing also [2].

flow model, because consideration of the complete 3-dimensional flow process is too demanding. In spite of the simplified two-dimensional flow model, for the four special cases mentioned above typical angle of attack distributions may be assigned, which are already known from measurement or calculation. Through superposition of known angle of attack distributions and the corresponding derivatives, the derivatives may be determined for cases not yet treated. Thus, estimates of interesting effects are possible without the need for new calculations or measurements of the desired derivatives.

3.2 Dead time effects as a result of angle of attack and downwash delays.

Case 1. Determination of $c_{M\dot{\alpha}}$

If the angle of attack for the wing α_{FL} and for the horizontal tail surface α_H is increased, by a pitch change of the aircraft for instance, then the changed downwash arrives at the tail delayed by the time Δt. Taking a constant rate of change for the wing angle of attack, then we have

$$\alpha_{FL} = \dot{\alpha} t. \tag{3}$$

The angle of attack for the tail is, for the stationary case and with neglect of the downwash delay on the tail surface:

$$\alpha_{H_o} = (1 - \varepsilon)\,\alpha_{FL_o}. \tag{4}$$

If the downwash delay is considered, then the angle of attack deviates from the fixed angle α_{H_o} by $\Delta\alpha_H$.

The relations can be seen from Figure 3. For $t > \Delta t$:

$$\Delta\alpha_H = \alpha_{FL}\Big|_{t=\Delta t} - \alpha_H(\text{Fixed})\Big|_{t=\Delta t} = \dot{\alpha}\Delta t - (1 - \varepsilon)\,\dot{\alpha}\Delta t = \varepsilon\dot{\alpha}\Delta t, \tag{5}$$

From Equations (5) and (1), the additional lift at the tail surface because of

---

[4] The downwash gradient ε at the horizontal tail surfaces is less than one for fixed-wing aircraft.

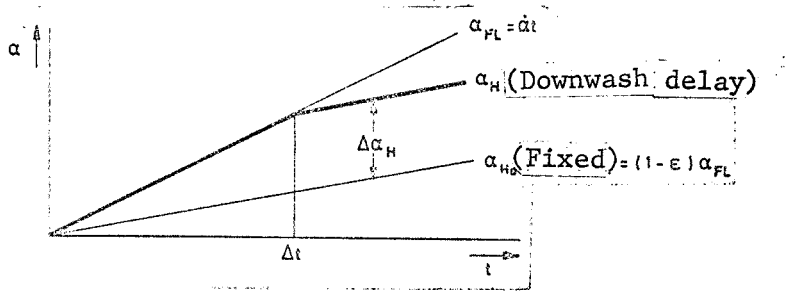

Figure 3

the downwash delay is

$$\Delta c_{AH} = c_{A\alpha H} \; \Delta\alpha_H = c_{A\alpha H} \, \varepsilon \, \frac{r_H}{V_o} \, \dot{\alpha} \; . \tag{6}$$

Partial differentiation with respect to $\dot{\alpha} l_\mu / V_o$ gives

$$\frac{\partial c_{AH}}{\partial(\frac{\dot{\alpha} l_\mu}{V_o})} = c_{A\alpha H} \, \varepsilon \, \frac{r_H}{l_\mu} = c_{A\dot{\alpha}H} \; . \tag{7}$$

If the derivative $c_{A\dot{\alpha}H}$ according to Appendix I is applied to the whole aircraft, then

$$c_{A\dot{\alpha}} = \frac{\partial c_A}{\partial(\frac{\dot{\alpha} l_\mu}{V_o})} = \frac{F_H}{F} \left(\frac{V_{H_o}}{V_o}\right)^2 \frac{r_H}{l_\mu} \, c_{A\alpha H} \, \varepsilon \tag{8}$$

and correspondingly /14

$$c_{M\dot{\alpha}} = \frac{\partial c_M}{\partial(\frac{\dot{\alpha} l_\mu}{V_o})} = - \frac{F_H}{F} \left(\frac{V_{H_o}}{V_o}\right)^2 \left(\frac{r_H}{l_\mu}\right)^2 c_{A\alpha H} \, \varepsilon \; . \tag{9}$$

This determination of $c_{M\dot{\alpha}}$ is generally known. The differentiation at this point should provide an introduction for the following differentiations, so that differences will be clearly visible.

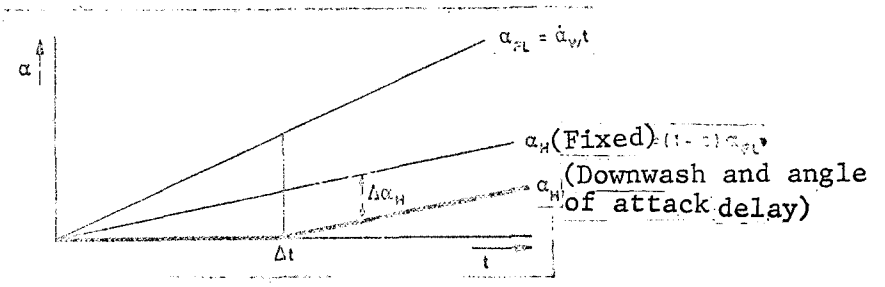

Figure 4

Case 2: Determination of $c_{M\dot{\alpha}w}$

If an aircraft flies into a vertical gust, a change in attack angle α_w occurs first at the wing and then, with a time delay Δt, together with the changed downwash, at the horizontal tail surfaces. If a constant rate of change for the angle of attack at the wing is assumed, then the equation corresponding to (3) applies:

$$\alpha_{FL} = \dot{\alpha}_w t \quad . \tag{10}$$

The fixed angle of attack change α_H for the tail results again from Equation (4).

Consideration of the delay of angle of attack and downwash shows that the angle of attack for the tail differs from the fixed angle α_H by $\Delta\alpha_H$. The relations can be seen in Figure 4. For the case where $t > \Delta t$: /15

$$\Delta\alpha_H = -\alpha_H(\text{fixed})\Big|_{t=\Delta t} = -(1-\varepsilon)\dot{\alpha}_w \Delta t \quad . \tag{11}$$

The further development is analogous to the differentiation of $c_{M\dot{\alpha}}$

$$\Delta c_{AH} = -c_{A\alpha H}(1-\varepsilon)\frac{F_H}{V_o}\dot{\alpha}_w \quad . \tag{12}$$

According to Appendix I, the partial differentiation with respect to $\frac{\dot{\alpha}_w l_\mu}{V_o}$

gives for the whole aircraft

$$c_{A\dot{\alpha}_w} = \frac{\partial c_A}{\partial\left(\frac{\dot{\alpha}_H l_\mu}{V_o}\right)} = -\frac{F_H}{F}\left(\frac{V_{H_o}}{V_o}\right)^2 \frac{r_H}{l_\mu}\, c_{A\alpha H}\,(1-\varepsilon), \tag{13}$$

$$c_{M\dot{\alpha}_w} = \frac{\partial c_{My}}{\partial\left(\frac{\dot{\alpha}_H l_\mu}{V_o}\right)} = \frac{F_H}{F}\left(\frac{V_{H_o}}{V_o}\right)^2 \left(\frac{r_H}{l_\mu}\right)^2 c_{A\alpha H}\,(1-\varepsilon). \tag{14}$$

Comparison with Equations (8) and (9) shows that $c_{A\dot{\alpha}}$ and $c_{M\dot{\alpha}}$ are contained in $c_{A\dot{\alpha}_w}$ and $c_{M\dot{\alpha}_w}$.

Further, if the relations for

$$c_{Ay} = \frac{F_H}{F}\frac{V_{H_o}}{V_o}\frac{r_H}{l_\mu}\, c_{A\alpha H} \tag{A2.4*}$$

and

$$c_{My} = -\frac{F_H}{F}\frac{V_{H_o}}{V_o}\left(\frac{r_H}{l_\mu}\right)^2 c_{A\alpha H} \tag{A2.4}$$

are taken from Appendix II, and V_{H_o}/V_o set equal to 1, Equations (13) and (14) /16 simplify to:

$$c_{A\dot{\alpha}_w} = c_{A\dot{\alpha}} - c_{Ay} = c_{Ay}\left(\frac{c_{M\dot{\alpha}}}{c_{My}} - 1\right) \tag{15}$$

$$c_{M\dot{\alpha}_w} = c_{M\dot{\alpha}} - c_{My} = -c_{My}(1-\varepsilon) \tag{16}$$

The $c_{M\dot{\alpha}w}$-effect will be differentiated with a further method which is particularly applicable for flying wings. Both effects, $c_{M\dot{\alpha}}$ and $-c_{My}$ may be clearly explained in this way. The distribution of the angle of attack over a wing (in the thrust direction) after the aircraft has flow into a ramp-formed vertical gust is shown in Figure 5a. They may be divided into elementary, generally known angle of attack distributions, for which a corresponding moment distribution can be assigned.

The constant portion leads to $c_{M\alpha}$; the variable portion $c_{M\dot{\alpha}w}$ can be broken /17 down further into $c_{M\dot{\alpha}}$ and $-c_{My}$, corresponding to Figure 5 b - d.

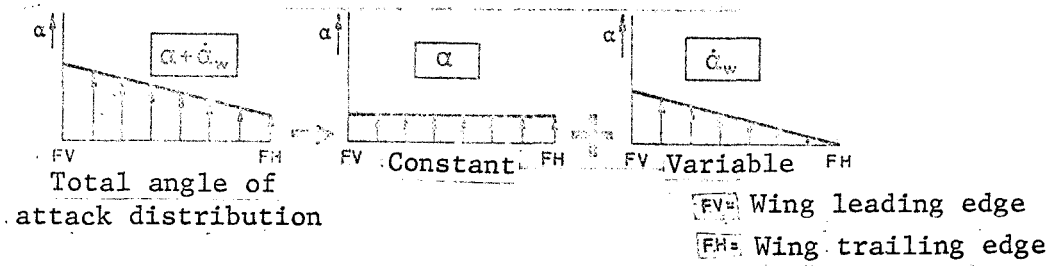

Figure 5a

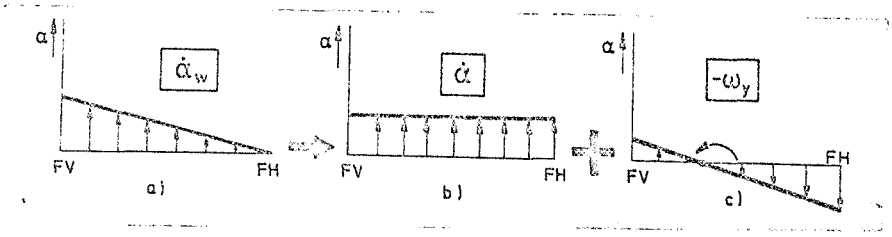

Figure 5 b, c, d

The angle of attack distribution in Figure 5d resembles that which results from a negative rotation in pitch (down-pitch, ω_y negative). (See Appendix II)

The differentiation leading to Equation (16) applies not only for aircraft with tail assemblies, but also for flying wings.

Of the two parts of the $\dot{\alpha}_w$ effect on the longitudinal moment, $-c_{My}$ derives from a delay in the angle of attack, and $c_{M\dot{\alpha}}$ from the downwash delay, as is to be seen from Figure 5 and Equation (16).

W. W. Phillips and C. C. Kraft [7] arrived at similar views on the basis of a method significantly different from that used here. B. Etkin [1] has derived the following relation for a sinusoidal gust perturbation:

$$c_{M\dot{\alpha}_w} = -c_{My} \ .$$

In this relation only the angle of attack delay is considered, and not the downwash delay. If the downwash delay is also considered for a sinusoidal gust perturbation, this leads to the same result as for a ramp-formed gust perturbation in Equation (16).

3.3 Dead time effects as a result of thrust velocity delays

Case 3: Determination of $c_{M\dot{u}}$

If the thrust velocity changes simultaneously at the wing and tail according to a ramp function $\Delta V = \dot{u}t$ corresponding to Figure 6, then the increased downwash arrives at the tail delayed by the time Δt, since it can only arrive at the tail with the initial vortex from the wing[5]. Since the additional velocity $\Delta V = \dot{u}t$ is small in relation to the constant thrust velocity V_o, the approximation of Equation (17) applies. Thus the delay time Δt can be assumed constant: /18

$$\Delta t = \frac{r_H}{V_o + \dot{u}t} \approx \frac{r_H}{V_o} \quad . \tag{17}$$

Because of the downwash delay, with a ramp-formed increase of the thrust velocity at the tail (Figure 6) the downwash velocity is smaller by

$$\Delta W_H = W_{Ho}|_{t=\Delta t} = \alpha_{aw} \Delta V \tag{18}$$

than in the fixed case. But since ΔV must be small with respect to V_{Ho}, the change of downwash angle $\Delta\alpha_{aw}$ due to downwash delay remains negligibly small (Figure 7). The derivatives $c_{M\dot{\alpha}}$ and $c_{M\dot{u}}$ describing a thrust

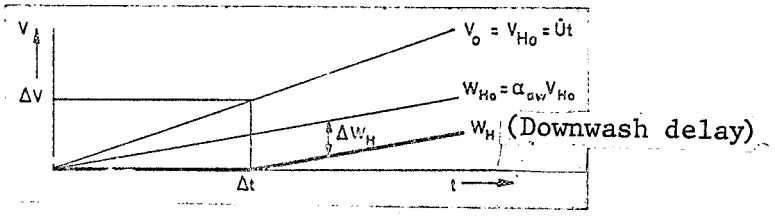

Figure 6

[5] Changes of the thrust velocity at the wing and tail as a result of changes in air speed do not result in a fixed change in the angle of attack at the tail, since the circulation at the wing and thus the downwash velocity W_{Ho} at the tail are proportional to the thrust velocity. Thus the downwash angle α_{awo} remains constant as the ratio of thrust velocity to downwash velocity (see Figure 7).

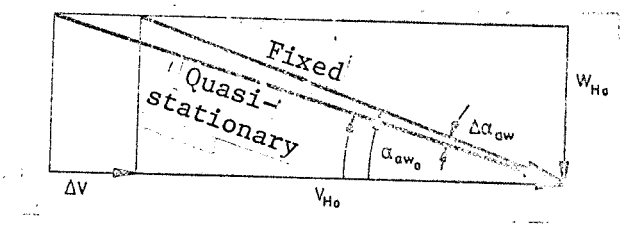

Figure 7

velocity delay can likewise be neglected.

Case 4: Determination of $c_{M\dot{u}w}$ /19

If, on the other hand, a plane flies into a horizontal gust, the increase of thrust velocity U_w occurs first on the wing and then, time-delayed by Δt, on the tail (Figure 8).

A thrust velocity delay leads, in contrast to the stationary case, to a thrust velocity at the tail which is smaller by ΔV:

$$\Delta V = -\frac{V_{H_o}}{V_o}\dot{U}_w\Delta t = -\frac{V_{H_o}}{V_o}\dot{U}_w\frac{r_H}{V_o} \quad . \tag{18}$$

The different thrust velocity at wing and tail in the stationary condition is considered through the term V_{H_o}/V_o. The total lift on the tail surface then becomes:

$$A_H = \frac{\rho}{2} F_H \left(V_{H_o} + \Delta V_H\right)^2 c_{AH_o} \quad . \tag{19}$$

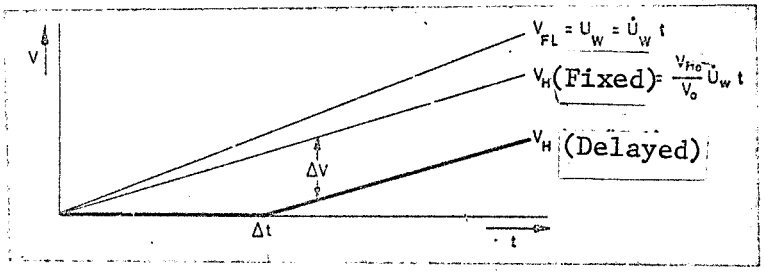

Figure 8

Since the change in the thrust velocity through gusts must be relatively small, ΔV_H^2 may be neglected as the square of a small value.

$$A_H = \frac{\rho}{2} F_H V_{H_o}^2 \left(1 + 2 \frac{\Delta V_H}{V_{H_o}}\right) c_{AH_o}. \tag{20}$$

Since one can assume that the changes of thrust velocities at the wing ΔV and at the tail ΔV_H are proportional to the fixed velocities, therefore /20

$$\frac{\Delta V}{V_o} = \frac{\Delta V_H}{V_{H_o}}, \tag{21}$$

With Equation (18), this leads to

$$A_H = \frac{\rho}{2} F_H V_{H_o}^2 c_{AH_o} \left(1 - 2 \frac{r_H}{V_o^2} \frac{V_{H_o}}{V_o} \hat{U}_w\right). \tag{22}$$

The partial differentiation of Equation (22) with respect to $U_w l_\mu / V_o^2$ gives:

$$\frac{\partial A_H}{\partial \left(\frac{U_w l_\mu}{V_o^2}\right)} = -2 \frac{V_{H_o}}{V_o} \frac{r_H}{l_\mu} \frac{\rho}{2} F_H V_{H_o}^2 c_{AH_o}. \tag{23}$$

With the recalculations from the tail assembly to the entire aircraft from Appendix 1, then:

$$c_{A\hat{U}_w} = \frac{\partial c_A}{\partial \left(\frac{U_w l_\mu}{V^2}\right)} = -2 \frac{F_H}{F} \left(\frac{V_{H_o}}{V_o}\right)^3 \frac{r_H}{l_\mu} c_{AH_o}, \tag{24}$$

$$c_{M\hat{U}_w} = \frac{\partial c_M}{\partial \left(\frac{U_w l_\mu}{V^2}\right)} = 2 \frac{F_H}{F} \left(\frac{V_{H_o}}{V_o}\right)^3 \left(\frac{r_H}{l_\mu}\right)^2 c_{AH_o}. \tag{25}$$

With the relationships from Appendix 2: /21

$$\frac{F_H}{F} \frac{V_{H_o}}{V_o} \frac{r_H}{l_\mu} = \frac{c_{Ay}}{c_{A\alpha H}}, \tag{A2.4*}$$

$$-\frac{F_H}{F} \frac{V_{H_o}}{V_o} \left(\frac{r_H}{l_\mu}\right)^2 = \frac{c_{My}}{c_{A\alpha H}} \tag{A2.4}$$

and

$$\frac{V_{H_o}}{V_o} \approx 1$$

Equations (24) and (25) simplify to:

$$c_{A\dot{u}_w} = -2\frac{c_{AH_o}}{c_{A\alpha H}} c_{Ay} \tag{26}$$

$$c_{M\dot{u}_w} = -2\frac{c_{AH_o}}{c_{A\alpha H}} c_{My} \tag{27}$$

3.4 Summarizing remarks on the gust derivatives

The investigations carried out in Chapter 3.1 show for ordinary aircraft a simple relation of the quasi-stationary gust derivatives with the $\dot{\alpha}$- and ω_y- derivatives. These relations describe $\dot{\alpha}_w$-effects accurately enough for all wing-tail combinations. The $\dot{U}_w$-derivatives apply also for delta-flying wings with center of gravity locations $x_S/l_\mu > 0.6$ [2]. For rectangular wings the deviations of $c_{M\dot{u}w}$ are too large.

This relation applies basically for all wing shapes:

$$c_{A\dot{u}_w} = c_{A_o} \tag{28}$$

Statements on intermittent conditions can be made for simple flying wing forms with the help of the theory of slender bodies [3]. The calculations, not shown here because they are too extensive, show that the derivatives are frequency-dependent, so that the relation given in Equation (2) is no longer adequate. The most important result of these calculations on the intermittent conditions is that of the ratio of $c_{M\dot{\alpha}_w}$ to $c_{M\dot{u}_w}$, independent of the frequency and the wing configuration. /22

$$\frac{c_{M\dot{\alpha}w}}{c_{M\dot{u}w}} = \frac{c_{A\alpha}}{c_{A_o}} = \frac{c_{A\dot{\alpha}w}}{c_{A\dot{u}w}} \tag{29}$$

Since the values for $c_{M\dot{\alpha}w}$ and $c_{A\dot{\alpha}w}$ are known approximately for many cases, approximate solutions for $c_{M\dot{u}w}$ and $c_{A\dot{u}w}$ can be obtained by use of Equation (29). Equation (29) also shows that $c_{M\dot{u}w}$ has significance only for large values of c_{Ao}. This case occurs in the landing approach as well as in cruising

flight at very high altitudes.

3.5 Physical action of the dead-time effect

Through an increase in flow velocity at the wing because of vertical or horizontal gusts, the magnitude of the additional moment at the wing is increased, while the flow at the tail surface, and thus the tail life and tail moment remain unchanged for the first moment. The stationary balance of moments for the aircraft is thus perturbed.

An increase in angle of attack as the result of a gust, with a conventional aircraft $c_{M\dot{\alpha}}$ of the wing >0, $c_{M\alpha}$ for the tail <0, $c_{M\alpha}$ for the total <0 for static balance) always causes, because of the positive $c_{M\alpha}$ at the wing, a positive (up-pitch) additional moment of the whole aircraft.

With an increase in thrust velocity through a gust, the additional moment at the wing always has the same direction as the fixed wing moment. This direction depends on the trim condition. For instance, in the landing approach with flaps extended, if the fixed wing moment is negative, then the comparable tail moment must be positive, and thus the tail lift must be negative. An increase in the thrust velocity because of a gust gives an immediate negative (down-pitch) additional moment, until the additional air velocity at the wing has reached the tail. /23

The tail lift is a measure of the size and direction of the fixed wing moment insofar as the propellor or jet moments do not play a dominant role and the center of gravity of the aircraft is near the neutral point.

The tail makes a singificant contribution to the total moment only when the separation of the tail from the aircraft neutral point is sufficiently great. But then the added lift of the horizontal tail surface is negligibly small as part of the total lift and also $c_{A\dot{u}_w}$.

3.6 Region of validity for quasi-stationary derivatives

A quasi-stationary theory is valid only up to an upper frequency limit. With ramp-form gust perturbations a steady-state condition must be expected and the steepness of the ramp must not be too great.

Sears [8] has reported that the pitch moment parameters with stochastic changes in the angle of attack α_w as a result of gusts corresponding to Equation (2) can be described with accuracy within 5%, if the highest effective frequencies which occur are smaller than

$$\omega_g < \frac{2\pi U_o}{8\, l_\mu} \quad , \tag{30}$$

or if the effective gust wave lengths λ of the turbulence field are larger than eight times the mean wing chord l_μ

$$\lambda > 8\, l_\mu \tag{31}$$

According to (2), gust frequencies with $\omega > 5[s^{-1}]$ or corresponding gust wave lengths of $\lambda < 100$ [m] at a flight speed of $U_o \approx 80$ m s^{-1} provide only an insignificant portion (> 2%) of the root-mean-square gust velocity, and thus can be neglected. Thus the allowable upper limiting frequencies for both example aircraft (see Appendix 3) in the landing approach are above the frequency region for rapid oscillation of the angle of attack. These upper limiting frequencies are shown as frequency lines in the basic diagrams (Figures B3 and B4). The limiting value for high frequencies (initial slope, initial value) is attained for both aircraft below the upper limiting frequency. That means that the quasi-stationary viewpoint for intermittent gust derivatives is completely adequate for rigid aircraft and not too great flight speeds. /24

4. Effects of instantaneous gusts on the aircraft longitudinal motion

The action of the quasi-stationary gust derivatives determined in the previous sections will be shown for two typical transport aircraft. Aircraft A is a subsonic transport plane of the Boeing 707 type, and B is a supersonic transport of the Concord type. Only the landing configuration is considered

for both planes. The aircraft characteristics and derivatives are tabulated in Appendix 3.

The root loci (polar zero position allotment) of the eight gust transfer functions[6] show a strong dependence of the zero positions[7] on $c_{M\dot{\alpha}w}$ and $c_{M\dot{u}w}$. The zero positions of all eight transfer functions shift over a wide range of the root locus plane (see Figures B1 and B2) with variations of different parameters ($c_{M\dot{\alpha}}/c_{My}$ in $c_{M\dot{\alpha}}$ and c_{AH_o} in $c_{M\dot{u}w}$). In all cases zero positions with positive real portions are possible. This indicates that no phase minimum system [9] is to be found and therefore all-pass and dead time effects can occur.

4.1 All-pass effects

/25

Two important all-pass effects can be seen in Figures B6 and B8 in $\vartheta/\alpha w$ and ϑ/u_w. The initial pitch motion proceeds exactly opposite to that which one would expect without the non-steady effect. Both all-pass effects will be physically clarified in the following.

The initial slope of the transfer function for a thrust change after a vertical gust is, according to [2]

$$\lim_{t\to 0} \frac{\omega_y}{\alpha_w} = \frac{c_{M\dot{\alpha}} + c_{M\dot{\alpha}T}}{i_y \; t_a} = \frac{2\, c_{M\dot{\alpha}} - c_{MX}}{i_y \; t_a} . \tag{32}$$

This limiting value is positive in the normal case. After a positive attack-angle gust (vertical gust from below) there occurs at first a positive (up-pitch) pitch angle rate (Figures B6 and B8). But a down-pitch of the aircraft is to be expected, because the system attempts to compensate for the increased angle of attack through decrease in the thrust angle. If the non-steady effects remain ineffective, this expected behavior occurs for the initial slope.

[6] Dependence of the four motion magnitudes α, γ, ϑ, and u on both perturbation magnitudes α_w and u_w.

[7] The common denominator of the transfer system is independent of the perturbation magnitude matrix [2].

In Section 3.5, the physical explanation for the up-pitching behavior is a result of the non-steady flow processes. If c_{My} is large enough, the all-pass effect shows itself to be quite effective (Aircraft B in Figure B 8). Through the all-pass effect the action of vertical gusts on the thrust angle is reduced, especially in the frequency region which lies between phygoid and rapid α-oscillation (basic diagram, Figure 4, $\frac{\vartheta}{w_{aw}}$=). The phase rotation of 90° in contrast to the case with $c_{M\dot{\alpha}w}$ is not even effective at phygoid frequencies with aircraft B. This all-pass effect is so easily visible with aircraft B because c_{My} is relatively large and $c_{M\alpha}$ small, so that the normal reaction described above begins relatively late and allows the non-steady flow enough time to build up a positive thrust angle change, which is only later decreased. Therefore, this all-pass effect is always to be expected for aircraft with a strongly damped ($\varepsilon_D > 45°$) low-frequency (spring component $c_{M\alpha}$ small) α-oscillation. With aircraft A, on the other hand, this condition does not exist, and the action of the all-pass effect is correspondingly small.

Increase of the thrust velocity through a horizontal gust causes primarily /26
an increase in lift. The results of this are a vertical acceleration and with that an increased flight path angle γ as well as a decreased angle of attack, α. If the thrust moment and non-steady gust effects are negligible, an up-pitching thrust change causes a return to the original angle of attack. This up-pitching movement opposes a down-pitch moment as a result of the non-steady gust effects, because according to Section 3.5 and [2], the initial slope of the step solution for a thrust change after a horizontal gust is negative:

$$\lim_{t\to 0} \frac{\omega_y}{u_w} = \frac{c_{zA_o}}{i_y t_a} = -2 \frac{c_{AH_o}}{c_{A\alpha H}} \frac{c_{mT}}{i_y t_a} \quad . \tag{33}$$

Both these opposing motions are clearly recognizable with aircraft B (Figure B8, ϑ/u_w).

4.2 Dead time behavior as a result of all-pass effects

If a complex conjugate zero-point pair with positive real portion and a

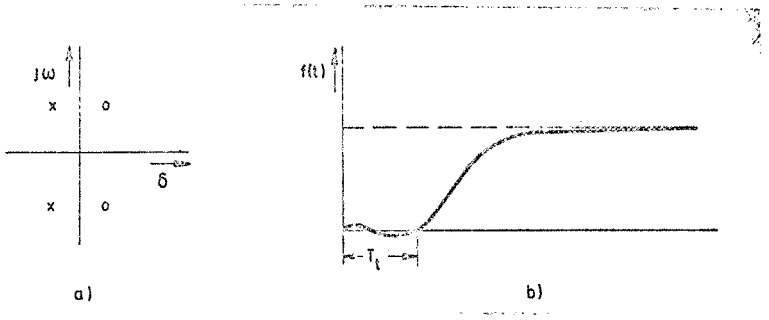

Figure 9

pair of poles lie symmetric to the imaginary axis of a root locus curve (Figure 9a), there occurs a special case of all-pass behavior (Figure 9b). With a step-formed perturbation, the magnitude of the motion reacts only after a "dead time", T_t. This approximation of a dead-time effect through an all-pass /27
effect was discussed on page 6 , footnote on the Pade approximation (Footnote 2). With aircraft B a dead time effect occurs in u/u_w with $c_{AH_o} = -1$ (Figure B8). In this case the complex conjugate zero point pair is the same as the pair of poles of the α-oscillation, up to the sign of the real component, (Figure B2). This dead time effect has a decisive influence on the choice of motion magnitudes to be controlled. For example, with aircraft A the flight path velocity would be an improper magnitude for measuring. Because of the dead time action of about six seconds a horizontal gust would be detected much too late for corresponding counter-measures to be taken, while other motion quantities, e.g. ϑ and γ would have reacted completely to the gust already. For the landing approach this would mean that because of a horizontal gust, the aircraft can depart significantly from the guidance beam before the flight speed changes.

4.3 Typical properties of $c_{M\dot{\alpha}}$ and $c_{M\dot{u}w}$

4.3.1 Variation of $c_{M\dot{\alpha}w}$ (Figures B2 and B3)

The quasi-stationary gust derivatives occur only in the meter coefficients of higher order [2]; for this reason, in the time domain they affect primarily the initial conditions, and in the frequency response curve, the course at

higher frequencies.

With both example aircraft, $c_{M\dot{\alpha}w}$ at frequencies below the phygoid eigenfrequency — considered separately from the angle of attack — has an amplitude-reducing action on all motion magnitudes. At higher frequencies, to be sure, the tendency is no longer uniform. For ϑ/α_w an amplitude reduction is visible in the frequency range between the eigen frequencies of phygoid and α-oscillation, while at higher frequencies the gust effect is slightly amplified again. The effect of $c_{M\dot{\alpha}w}$ on ϑ/α_w at higher frequencies remains small in spite of that, as the total amplitude of the gust spectrum is already very small (about 0.01 for $\omega = [10\ s^{-1}]$.

Since the reaction of the angle of attack α on gusts is very small (see α/α_w and α/u_w in Figures B3 to B8), each increase of the pitch angle ϑ leads to an increase of the flight path angle γ (red curve in Figure B6 and B8 in γ/α_w and γ/u_w). This has a very bad effect on ability to hold to the course- and altitude beams.

Through γ/α_w as well as through $\dot{\gamma}/\alpha_w$, $c_{M\dot{\alpha}w}$ affects only the frequency /28
range between the two eigen frequencies. The amplitudes in this frequency range would be large aside from that, and are further increased by $c_{M\dot{\alpha}w}$. On the other hand, u and $\dot{u}$ have through $c_{M\dot{\alpha}w}$ a gust-moderating effect over the entire frequency range. An effect of $c_{M\dot{\alpha}w}$ exists only at frequencies below the phygoid frequency, and to be sure, $c_{M\dot{\alpha}w}$ increases the gust effect.

The wing downwash on the horizontal tail surfaces diminishes the effect of $c_{M\dot{\alpha}w}$. The curves which consider the downwash (red) $c_{M\dot{\alpha}w} = c_{M\dot{\alpha}} - c_{My}$ thus always lie between the curves without downwash (blue) $c_{M\dot{\alpha}w} = -c_{My}$ and those with $c_{M\dot{\alpha}w} = 0$ (black). Since for both aircraft studied $c_{M\dot{\alpha}}$ is small in comparison with c_{My}, the effects of downwash on the reactions of these aircraft are relatively small.

4.3.2 Variation of $c_{M\dot{w}}$ (Figures B2 and B3)

In the region of the phygoid frequencies and below, the effect of $c_{M\dot{w}}$ on the gust solutions for the magnitudes of motion is relatively small. For the phygoid frequency, the effect of $c_{M\dot{w}}$ is exactly zero. For frequencies smaller than the phygoid frequency a positive $c_{M\dot{w}}$ (c_{AH_o} positive) has a slight amplitude-increasing result. For frequencies slightly over the phygoid frequency, the opposite is the case. However, a strong effect of $c_{M\dot{w}}$ is ascertainable in the frequency range of α-oscillation. A positive $c_{M\dot{w}}$ has the effect of increasing the amplitudes for the flight path motion quantities γ and u. For α and ϑ on the other hand, the amplitudes are weakened, because of the all-pass effects. A positive $c_{M\dot{w}}$ has a gust-moderating effect on the angle of attack α over the entire frequency range. On the other hand, the α-eigen frequency has a gust-strengthening effect on ϑ, independent of the sign of $c_{M\dot{w}}$.

Basically, this means that $c_{M\dot{w}}$ shows the greatest effect on ϑ and ω_y, but particularly at negative values of $c_{M\dot{w}}$ in the region of α-oscillation as a result of all-pass behavior (in the ordinary flight mode c_{AH_o} and thus $c_{M\dot{w}}$ are negative). The especially strong effect of $c_{M\dot{w}}$ on ϑ may be explained through the primary effect of the longitudinal moment of the longitudinal thrust angle. From the step solutions it is seen that the all-pass effects generated through $c_{M\dot{w}}$ under circumstances (aircraft A) cause a slight amplitude moderation, but the normal result is an increase in amplitudes and dead time effect. /29

5. Some effects of non-steady gust effects on flight control systems.

The stated properties of the frequency-dependent longitudinal moments caused by gusts can have a particularly destructive effect on control systems which are based on compensating action. This is, for example, the situation with a concept of the RAE for an automatic landing system (BLEU). If the undesirable stalling of the plane after a negative gust parallel to the flight path (wind from

behind) is compensated in this way, the decrease in thrust velocity causes the elevator to become deflected in a negative sense (pulled). Since this compensation superimposition can have a destabilizing effect [10], the magnitude of the feedback is largely defined. Consideration of the quasi-stationary moments can lead to significant change in the feedback amplification. This is at this time the reason that the results of simulation and flight study do not agree extensively.

The good properties of an automatic throttle system rest largely in clever compensation for gust effects. By means of one or more measured quantities, which are modified in a frequency-dependent manner by a computer, automatic throttle systems [11, 12] adjust the propulsive thrust so that the flight speed departs as little as possible from a preset control point. Most of the automatic throttle systems built so far work according to the following principle (Figure 10):

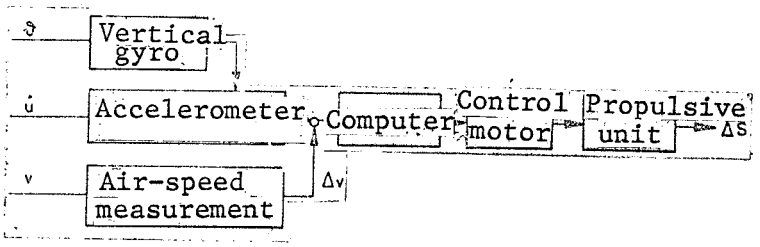

Figure 10

The thrust velocity V is measured by the air-speed indicator and the departure, /30
ΔV, from the present velocity is superimposed on the acceleration in the flight path direction, $\dot{u}$. In the accelerometer, a built-in part of the aircraft, the component of the acceleration of gravity in the direction of flight is compensated by the longitudinal thrust angle ϑ measured in the vertical gyro. A computer applies the superimposed acceleration and speed signal to the control motor, which adjusts the thrust of the propulsion unit. With higher frequency horizontal gusts, the thrust of the propulsion unit changes with the gust

frequency. This leads to undesirable attendant phenomena, such as engine howling and fluctuation of cabin pressure. By clever superimposition of $\dot{u}$ and V these gust sensitivities of the thrust adjustment at higher frequencies can be nearly repressed. According to Equation (33) (reference 2)

$$\dot{u} = -\frac{2c_{w_o}}{\mu_L t_a} u_w \tag{33}$$

a change of the thrust velocity $V = U_W$ is directly proportional to a change in acceleration. Equation (33) also shows, however, the dependence of the proportionality factor on flight position and gross weight. That means that the gust compensation can be ideal only for a definite flight condition and a fixed gross weight. This is nearly always the case in the landing approach.

This gust compensation process can fail for aircraft which are similar to the type B investigated and which show dead time behavior corresponding to that of Section 4.2, because the flight path acceleration $\dot{u}$ is delayed by about six seconds. The thrust velocity on the other hand is not delayed, so that the thrust fluctuation increases. In this case v and $\dot{u}$ would not be proper feedbacks to the controller.

6. Summary

Non-stationary gust effects have a significant influence on aircraft longitudinal motion. For vertical gusts, downwash delays have been considered along with delays in the angle of attack. For horizontal gusts, consideration of a delay in the thrust velocity develops new influences which are not to be neglected. These non-stationary gust effects, which in the sense of control technology show true dead time behavior, may be described with sufficient accuracy for the relatively low-frequency range of aircraft motions, using the quasi-stationary approach with simple equations: /31

$$c_{M\dot{u}_w} = c_{M\dot{\alpha}} \cdot c_{My}$$

$$c_{M\dot{u}_w} = -2\frac{c_{A_o}}{c_{A\alpha}} c_{My}$$

Non-steady statements can be derived for simple flying wing forms with the help of the theory of slender bodies. They show that the gust derivatives are frequency-dependent. In spite of that, the ration of $c_{M\dot{\alpha}w}$ to $c_{M\dot{w}w}$ remains independent of the wing configuration and the frequency.

$$\frac{c_{M\dot{\alpha}w}}{c_{M\dot{w}w}} = \frac{c_{A\alpha}}{c_{A_0}}$$

The quasi-stationary consideration method yields the great advantage of allowing the determination of gust derivatives with the help of other common aircraft characteristics, because for flight control problems it is always very difficult to get the necessary aircraft characteristics and nearly impossible to obtain additional new derivatives.

In all eight transfer functions, non-steady gust effects produce non-negligible all-pass effects (positive zero positions) which can have significant dead time effects. These dead time effects can have a decisive influence on the choice of motion quantities to be controlled. For example, with a plane of the Concorde type, the air speed would under certain conditions be an improper measure. As a result of the dead time effect of about six seconds, a horizontal gust would be detected much too late, so that no appropriate countermeasures could be taken, while other motion quantities such as the flight path angle or the longitudinal thrust angle would have already reacted completely to the gust. For the landing approach that would mean that as the result of a horizontal gust, the airplane can depart significantly from the guiding beam before the airspeed changes.

REFERENCES

1. Etkin, B. Dynamics of Flight, Stability and Control. J. Wiley and Sons, Inc., London, 1959.
2. Schänzer, G., Einfluss von verkoppelten instationären Böenstörungen auf die Flugzeuglängsbewegung (Effect of coupled non-steady gust perturbations on aircraft longitudinal motion). Dissertation accepted by the Technical University of Braunschweig, submitted 5 Nov 68.
3. Jones, R.T. Properties of low-aspect-ratio pointed wings at speed below and above the speed of sound NACA Rep. Nr. 835, 1946.
4. Perron, O., and B.G. Teubner, Die Lehre von den Kettenbrüchen (The theory of continued fractions), Stuttgart, 1957.
5. Giloi, Lauber, Analogrechnen (Analog computation). Springer Verlag, 1963.
6. Hamel, P. Beiträge zum Einfluss der Tragflächeninterferenz auf die Längsbewegung eines flexiblen Körpers (Contributions to the effect of wing interference on the longitudinal motion of a flexible body). Dissertation, Technical University of Braunschweig, 1968.
7. Phillips, W.H., and C.C. Kraft, Jr. Theoretical study of some methods for increasing the smoothness of flight through rough air, NACA TN 2416, July, 1951.
8. Sears, W.R. Some Aspects of Non-Stationary Airfoil Theory and its Practical Application, J. Aero. Sci., Vol. 8, 1941.
9. Oppelt, W. Kleines Handbuch technischer Regelvorgänge (Small Handbook of Technical Control Processes), Verlag Chemie, 1964 (Fourth edition).
10. Brockhaus, R. Über die Verkopplung und den Einfluss von Allpasseigenschaften in speziellen Mehrgrössensystemen am Beispiel der Regelung der Flugzeuglängsbewegung im Landeanflug (On coupling and the influence of all-pass properties in special multi-value systems, with the example of control of aircraft longitudinal motion in the landing approach). DLR Report DLR FB 67-74, July, 1967.
11. Reerink. Vortriebsregler FVR 01 (Automatic throttle control system FVR 01). Fluggerätewerk Bodensee GmbH (Bodensee Aircraft Equipment, Inc.) TB 000229/67, January, 1967.
12. Smith Industries LTD: Smith Autothrottle System Publication No. SAV, 157.
13. Schlichting, H., and E. Truckenbrodt, Aerodynamik des Flugzeuges (Aerodynamics of Aircraft), Springer Verlag 1960/62, Volumes 1 and 2.

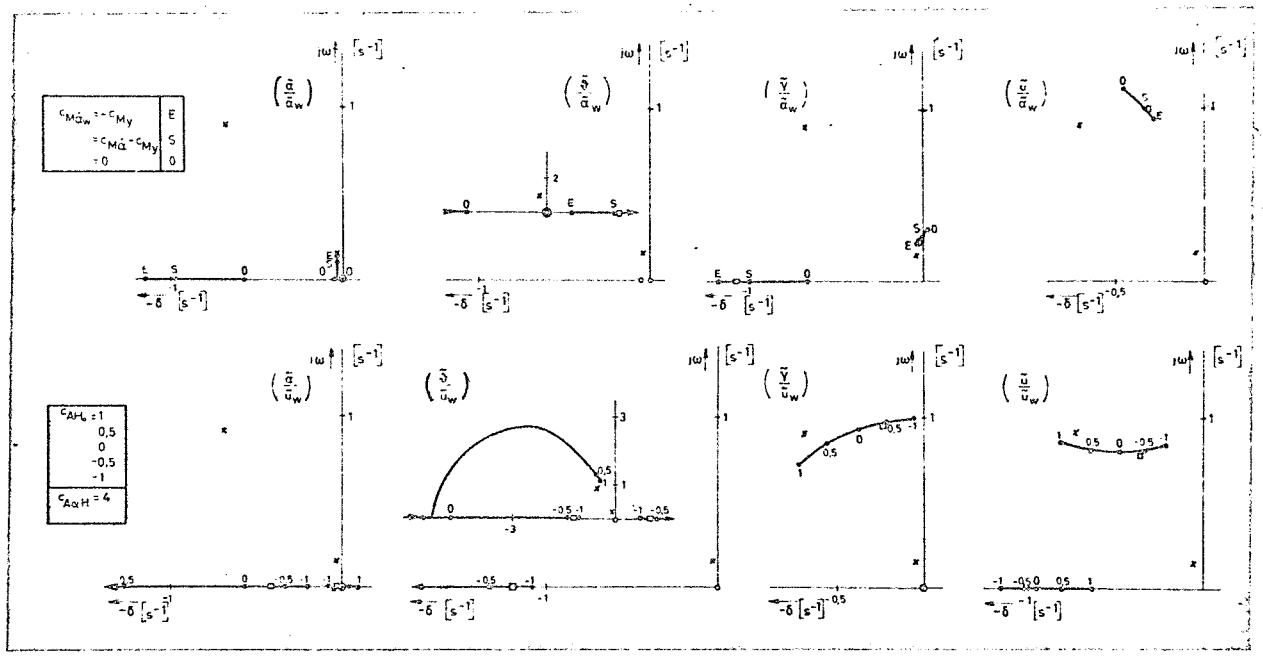

Figure B1 Root locus course with variation of $c_{M\dot{\alpha}_w}$ and $c_{M\dot{u}_w}$

$$c_{M\dot{\alpha}_w} = c_{M\dot{\alpha}} - c_{My}; \quad c_{M\dot{u}_w} = -2\,\frac{c_{AH_a}}{c_{A\alpha H}}\,c_{My}$$

Aircraft A

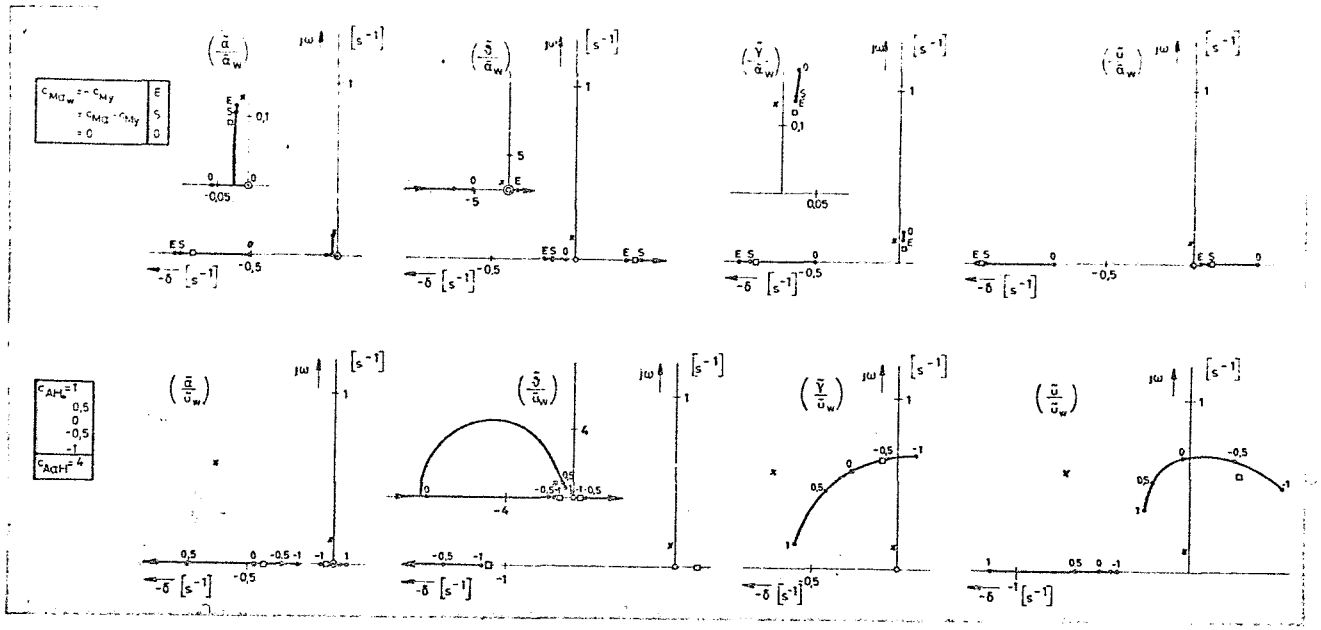

Figure B2 Root locus course with variation of $c_{M\dot{\alpha}_w}$ and $c_{M\dot{u}_w}$

$$c_{M\dot{\alpha}_w} = c_{M\dot{\alpha}} - c_{My} \; ; \qquad c_{M\dot{u}_w} = -2\,\frac{c_{AH_0}}{c_{A\alpha H}}\,c_{My}$$

Aircraft B

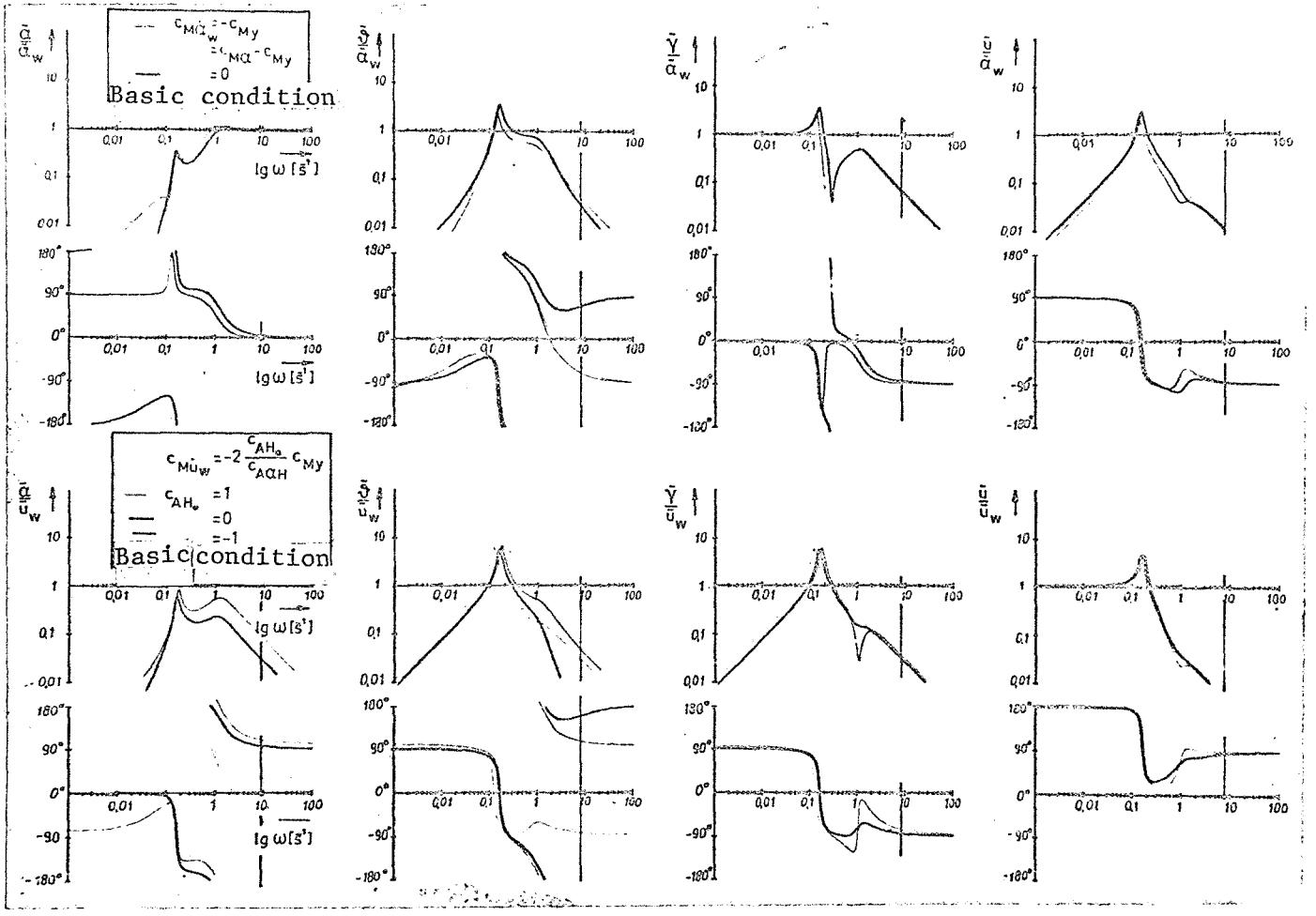

Figure B3 Fundamental diagrams for variations of $c_{M\dot{\alpha}_w}$ and $c_{M\dot{u}_w}$

Aircraft A

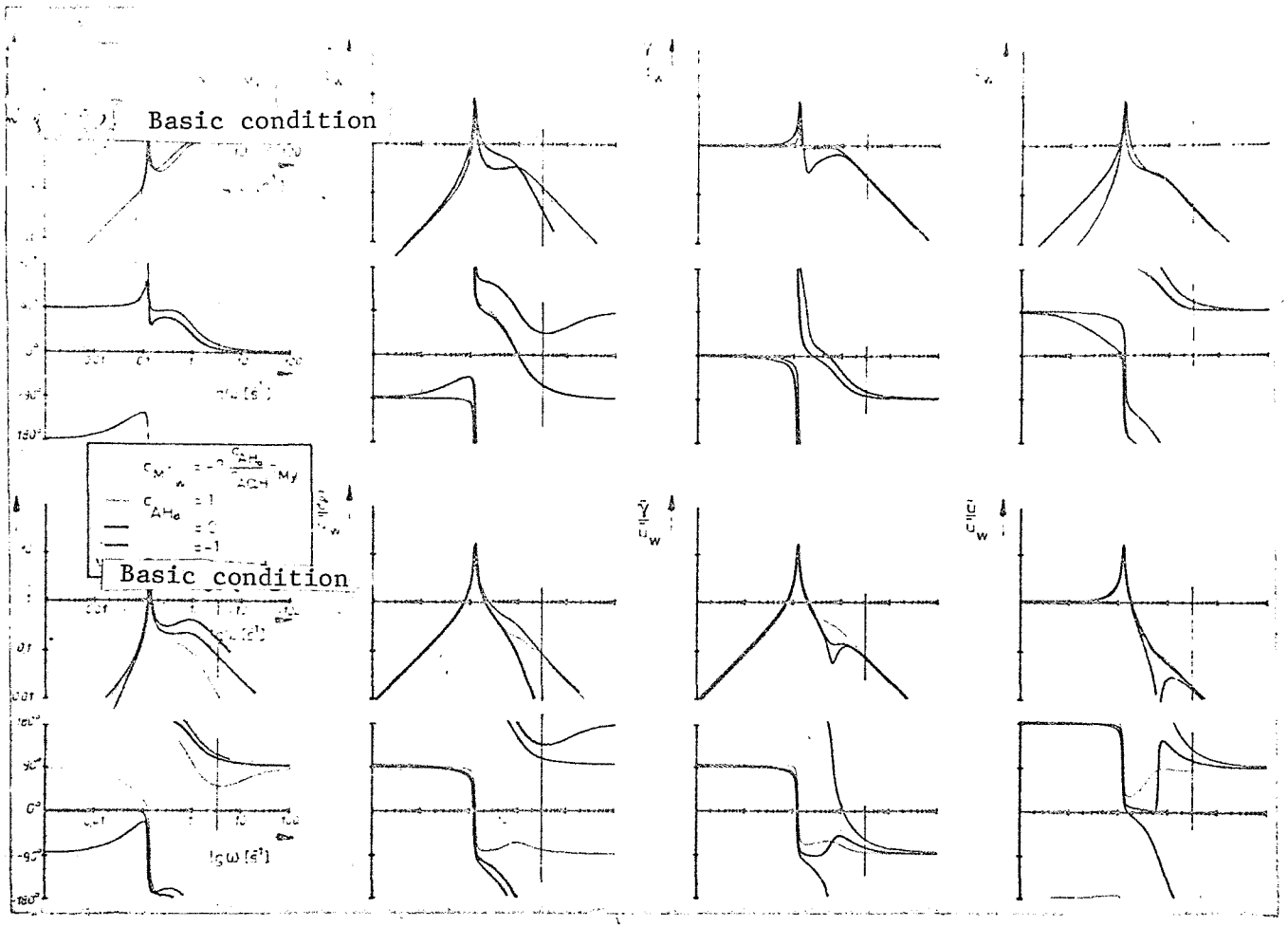

Figure B4 Fundamental diagrams for variation of $c_{M\dot{\alpha}_w}$ and $c_{M\dot{u}_w}$

Aircraft B

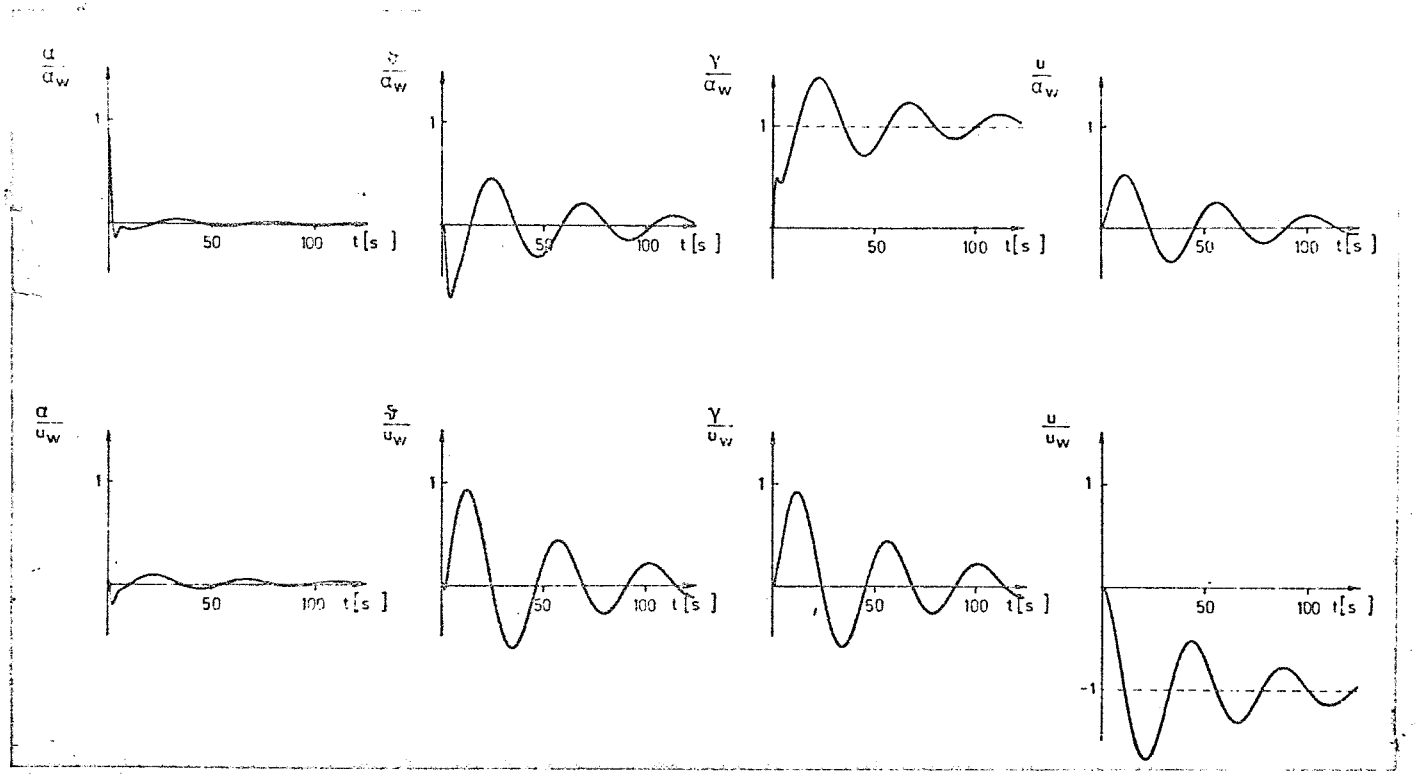

Figure B5 Transfer functions for the basic condition

Aircraft A

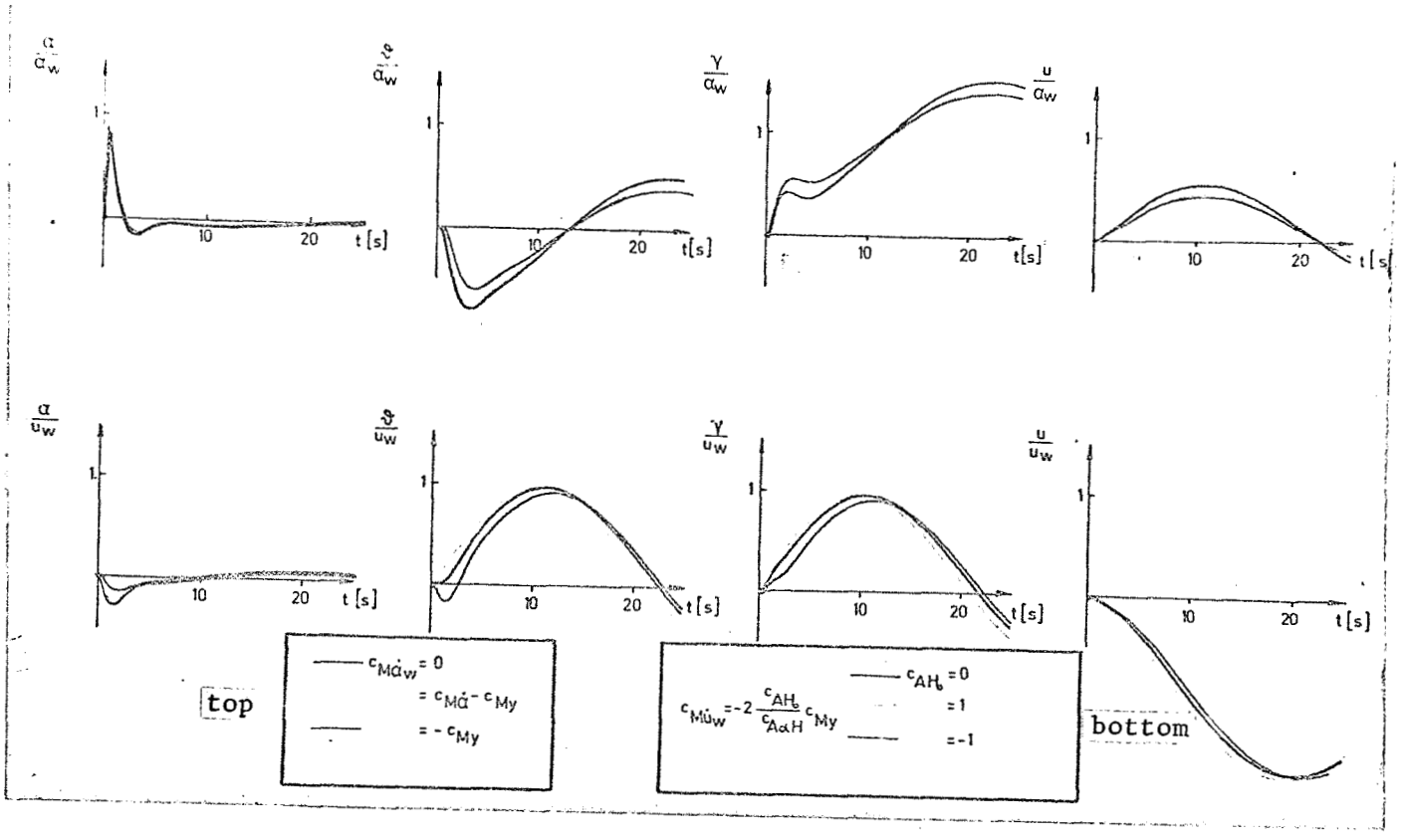

Figure B6 Transfer functions for variations of $c_{M\dot{\alpha}_w}$ and $c_{M\dot{u}_w}$

Aircraft A

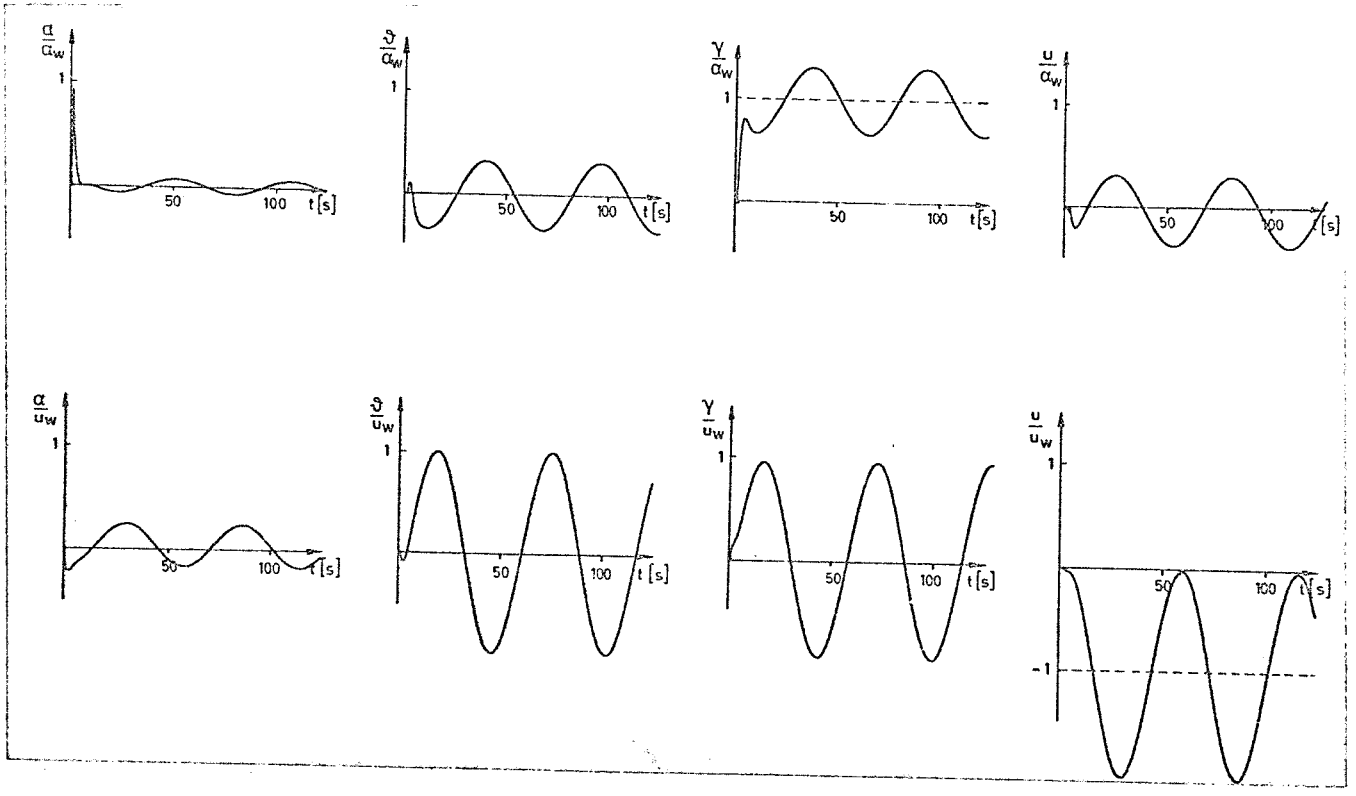

Figure B7 Transfer functions for the basic condition

Aircraft B

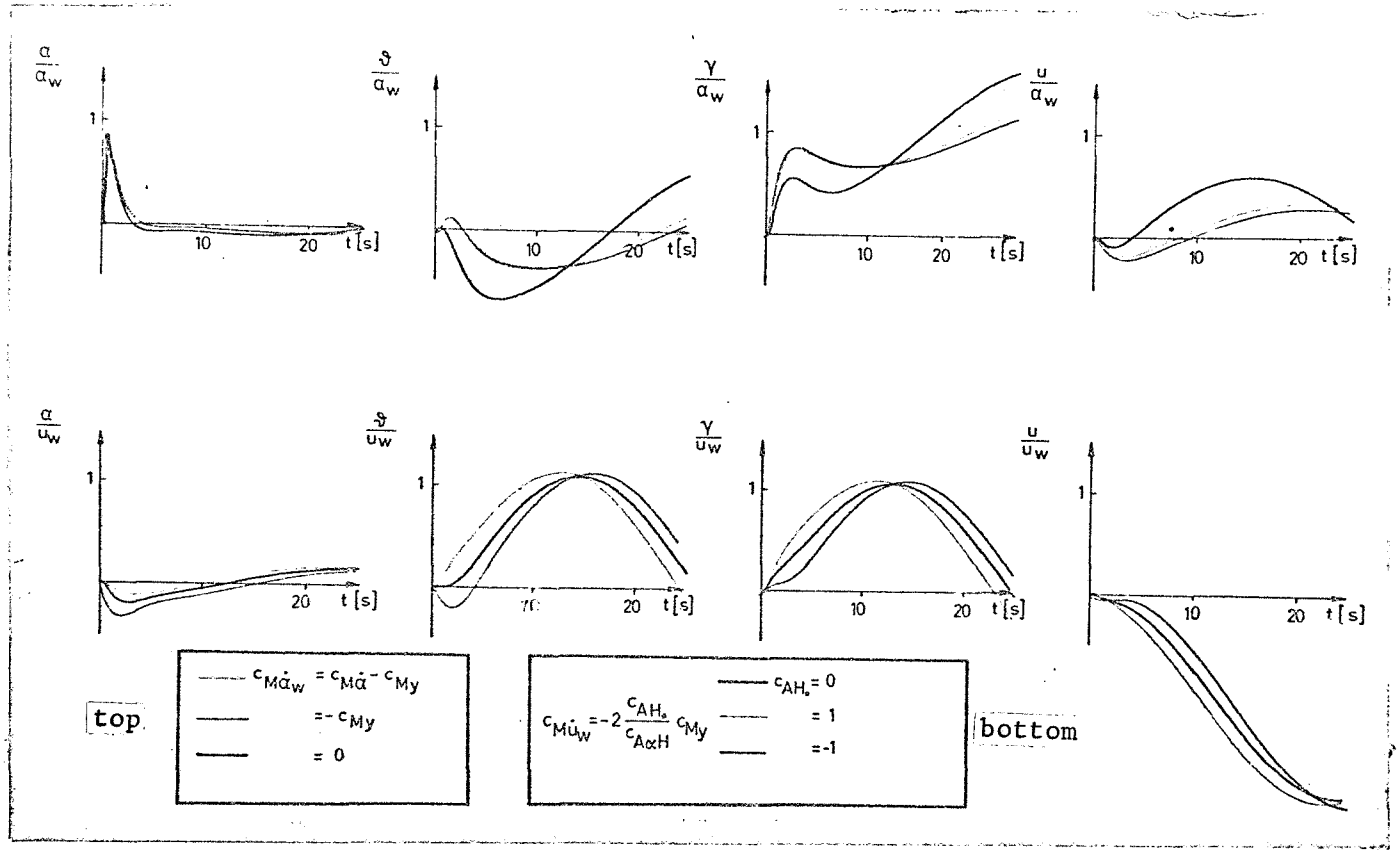

Figure B8 Transfer functions for variations of $c_{M\dot{\alpha}_w}$ and $c_{M\dot{u}_w}$

Aircraft B

APPENDIX 1

/42

Recalculation of the horizontal tail surface parameters for the total aircraft

Let the tail lift be

$$A_H = \frac{\varrho}{2} V_H^2 F_H c_{AH} \,. \tag{A1.1}$$

Correspondingly, for the total aircraft, we have

$$A = \frac{\varrho}{2} V^2 F c_A \,, \tag{A1.2}$$

$$M = \frac{\varrho}{2} V^2 F l_\mu c_M \,. \tag{A1.3}$$

If r_H is the distance of the tail surface neutral point from the center of gravity, then the horizontal tail surface produces the moment

$$M = - r_H A_H \,. \tag{A1.4}$$

The contribution of the tail to the total life and moment then is

$$\Delta c_A = \frac{F_H}{F} \cdot \left(\frac{V_H}{V}\right)^2 c_{AH} \,, \tag{A1.5}$$

$$\Delta c_M = - \frac{F_H}{F} \left(\frac{V_H}{V}\right)^2 c_{AH} \frac{r_H}{l_\mu} = - \frac{r_H}{l_\mu} \Delta c_A \,. \tag{A1.6}$$

APPENDIX 2

/43

Calculation of the quasi-stationary tail surface component of c_{My} [13]

If an aircraft is turned in a pitching motion (around the y-axis) with a constant angular velocity ω_y, the additional angle of attack at the tail is, according to Figure A.2.1:

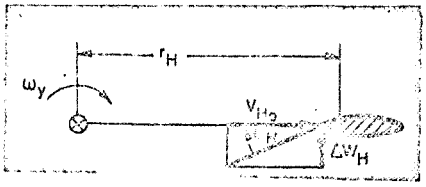

Figure A2.1

$$\Delta w_H = \omega_y r_H \,, \tag{A2.1}$$

$$\Delta\alpha_H = \frac{\omega_y r_H}{V_{H_o}} \,. \tag{A2.2}$$

The separation between the y-axis and the tail surface neutral point is r_H. This separation is about the same as the separation between the wing and tail neutral points for aircraft with not too small tail length and too great a rear location of the center of gravity.

According to Appendix 1, this equation applies for the additional moment parameter of the total aircraft as a result of a pitch angular velocity ω_y:

$$\Delta c_M = -\frac{F_H}{F}\left(\frac{V_{H_o}}{V_o}\right)^2 \frac{r_H}{l_\mu}\, c_{A\alpha H}\, \frac{\omega_y r_H}{V_{H_o}} \,. \tag{A2.3}$$

Through partial differentiation of (A2.3) with respect to $\frac{\omega_y \cdot l_\mu}{V_0}$, one obtains the derivative

$$c_{My} = \frac{\partial c_M}{\partial\left(\frac{\omega_y \cdot l_\mu}{V_o}\right)} = -\frac{F_H}{F}\frac{V_{H_o}}{V_o}\left(\frac{r_H}{l_\mu}\right)^2 c_{A\alpha H} \tag{A2.4}$$

APPENDIX 3

Aircraft Examples

Two aircraft were investigated, which show typical reactions to gust perturbations. For both aircraft, the flight condition for the landing approach is chosen, because gusts are of special importance for the landing approach.

Aircraft A is a transport aircraft with high subsonic speed, large moment of inertial, and relatively high aspect ratio. It corresponds generally to the Boeing 707 type.

Aircraft B is a supersonic transport aircraft with a slender "OGEE" wing, very small aspect ratio, and is of the Concorde type. Since the mean wing chord l_μ is large, the derivatives which are derived with respect to l_μ appear small. Because of the unstable phygoid, the gust effect in the region of the phygoid frequency is easily visible.

For both aircraft, the landing configuration is used here; the landing gears are extended, and with aircraft A, the flaps are also extended.

	Designation	Dimension	Aircraft A	Aircraft B
Gross weight	G	Kp	$9{,}4 \cdot 10^4$	$8{,}2 \cdot 10^4$
Moment of inertia around the lateral axis	I_y	Kp m s^2	$7{,}5 \cdot 10^5$	$8{,}55 \cdot 10^5$
Air speed	U_o	m s^{-1}	73,4	81,8
Designed wing chord	l_μ	m	6,93	27,66
Wing surface	F	m^2	268,7	358,3
Thrust radius	r_σ	m	1,0	2,0
Derivatives	c_{A_o}		1,035	0,556
	c_{W_o}		0,154	0,127
	$c_{A\alpha}$		4,48	3,32
	$c_{W\alpha}$		0,345	1,275
	$c_{M\alpha}$		-2,62	-0,03
	c_{My}		-7,35	-0,289
	$c_{M\dot{\alpha}}$		-1,20	-0,088